TRANSPORT COEFFICIENTS FOR A SLOW FERMI-PARTICLE MOTION

J.P. Blocki[1] and A.G. Magner[2]

[1] *National Center for Nuclear Research, Otwock 05-400, Poland*

[2] *Institute for Nuclear Research, Kyiv, Ukraine*

19th Nuclear Physics Workshop "Marie and Pierre Curie"
Kazimierz Dolny, Poland, 26.09-30.09, 2012

Plan of talk

1. INTRODUCTION. Quantum-classical correspondence in the nuclear collective dynamics

2. RESPONSE THEORY AND TRANSPORT COEFFICIENTS

3. SEMICLASSICAL FRICTION AND INERTIA

4. DISCUSSIONS OF THE RESULTS

5. CONCLUSIONS

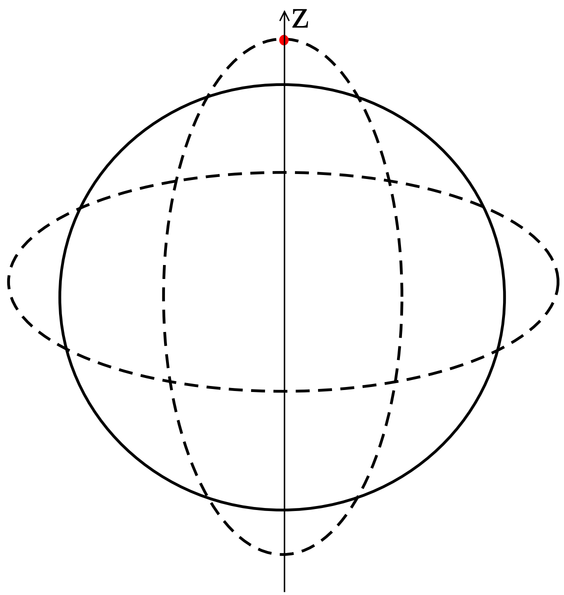

1) $\frac{dE}{dt} = \rho\bar{v}\oint \dot{n}^2 d\sigma$

WALL FORMULA, Swiatecki et al. 1977,78

2)**ORDER-CHAOS, POINCARE SECTIONS LYAPUNOV EXPONENTS**, Swiatecki, Blocki et al. 1995-1999

3) **QUANTUM AND CLASSICAL RESULTS FOR EXCITATION ENERGY**, Swiatecki, Blocki, Skalski et al. 1995-2007;

Blocki, Yatsyshyn, Magner, 2010-11, **FOR 10-20 OSC. PERIODS:**

$$dE/dt = M\dot{\alpha}\ddot{\alpha} + \gamma\dot{\alpha}^2 \qquad \Rightarrow \qquad < dE/dt >= \gamma\omega^2\alpha^2/2$$

4)**SEMICLASSICAL FRICTION AND INERTIA OF ONE-BODY COLLECTIVE DYNAMICS**, Koonin, Randrup
Gutzwiller POT: Gzhebinsky, Magner, Fedotkin, 2007
SMOOTH FRICTION: LOCAL WALL FORMULA)

5) **QUANTUM AND SEMICLASSICAL FRICTION AND INERTIA, NONLOCAL TRAJECTORY CORRECTIONS WITHIN POT**

2. RESPONSE THEORY AND TRANSPORT COEFFICIENTS

COLLECTIVE RESPONSE to $V_{\rm ext}(t) = \hat{F}\alpha^{\omega}_{\rm ext}e^{-i\omega t}$

$$\delta\langle\hat{F}\rangle_{\omega} = -\chi_{\rm coll}(\omega)\alpha^{\omega}_{\rm ext}, \quad \hat{F}({\rm r}) = \left(\frac{\partial V}{\partial\alpha}\right)_{\alpha=0} = -V_0 R\,\delta(r-R)\,Y_{L0}(\theta)$$

DYNAMICAL NUCLEAR SURFACE VIBRATIONS

$$\delta R(\theta,\alpha) \propto R\alpha(t)Y_{L0}(\theta), \qquad \alpha(t) = \alpha_{\omega}e^{-i\omega t}$$

SELFCONSISTENCY CONDITION, Bohr & Mottelson (1975)

$$\delta\langle\hat{F}\rangle_{\omega} = \kappa\,\delta\alpha_{\omega} \qquad \text{with the coupling constant } \kappa$$

$$\chi_{\rm coll}(\omega) = \kappa\frac{\chi(\omega)}{\chi(\omega)+\kappa}, \qquad \left[\delta\langle\hat{F}\rangle_{\omega} = -\chi(\omega)\left(\delta\alpha_{\omega} + \alpha^{\omega}_{\rm ext}\right)\right]$$

STRENGTH FUNCTION $\qquad S(\omega) = \frac{1}{\pi}\,{\rm Im}\chi_{\rm coll}(\omega)$

TRANSPORT COEFFICIENTS, Hofmann et al. (1997,2008)

$$\frac{1}{\chi_{\rm coll}(\omega)} = \frac{1}{\chi^{\rm osc}_{\alpha\alpha}(\omega)} = \frac{1}{\chi_{\alpha\alpha}(\omega)} + \kappa = -M\omega^2 - i\gamma\omega + C$$

INTRINSIC TRANSPORT COEFFICIENTS in the limit $\omega \to 0$

$$\chi\,(\omega) = \chi(0) - i\gamma(0)\,\omega - M(0)\,\omega^2 + ..., \qquad \chi(0) = -\kappa - C(0)$$

$$C = [1 + C(0)/\chi(0)]\,C(0), \quad \gamma = [1 + C(0)/\chi(0)]^2\gamma(0)$$

$$M = [1 + C(0)/\chi(0)]^2\left[M(0) + \gamma^2(0)/\chi(0)\right]$$

INTRINSIC RESPONSE $\Longleftrightarrow$ GREEN'S FUNCTION

$$\chi(\omega) \propto \int_0^\infty {\rm d}\varepsilon\,{\rm n}(\varepsilon) \int {\rm dr}_1 \int {\rm dr}_2\,\hat{F}({\rm r}_1)\,\hat{F}({\rm r}_2)\,{\rm Im}G({\rm r}_1,{\rm r}_2;\varepsilon)$$

$$\times\left[\,G^*\,({\rm r}_1,{\rm r}_2;\varepsilon - \hbar\omega) + G\,({\rm r}_1,{\rm r}_2;\varepsilon + \hbar\omega)\right], \quad G = \sum_i \frac{\psi_i({\rm r}_1)\,\overline{\psi}_i({\rm r}_2)}{\varepsilon - \varepsilon_i + i\epsilon}$$

$$\gamma(0) = \left(\partial\chi(\omega)/\partial\omega\right)_{\omega=0}, \quad M(0) = (1/2)\left(\partial^2\chi(\omega)/\partial\omega^2\right)_{\omega=0}$$

4. SEMICLASSICAL FRICTION AND INERTIA (sph. box)

$$\gamma = \int_0^{\pi} \sin\psi d\psi P_n(\cos\psi)\,\gamma(\psi), \qquad \gamma(\psi) \propto \left(\partial^2 \mathrm{Im} G/\partial r_1 \partial r_2\right)^2_{S,F}$$

$$M = \int_0^{\pi} \sin\psi d\psi P_n(\cos\psi)\,M(\psi), \quad M(\psi) \propto \int_0^{\varepsilon_F} d\varepsilon \left(\frac{\partial^2 \mathrm{Im} G}{\partial r_1 \partial r_2} \frac{\partial^2}{\partial \varepsilon^2} \frac{\partial^2 \mathrm{Re} G}{\partial r_1 \partial r_2} \right)_S$$

GREEN'S FUNCTION (Gutzwiller, 1971) for $k_F R_0 \sim A^{1/3} >> 1$:

$$G(\mathbf{r}_1, \mathbf{r}_2; \varepsilon) = \sum_{CT} \mathcal{A}_{CT}(\mathbf{r}_1, \mathbf{r}_2; \varepsilon) \exp\left[\frac{i}{\hbar} S_{CT}(\mathbf{r}_1, \mathbf{r}_2; \varepsilon) - \frac{i\pi}{2}\mu_{CT} - \phi_d\right]$$

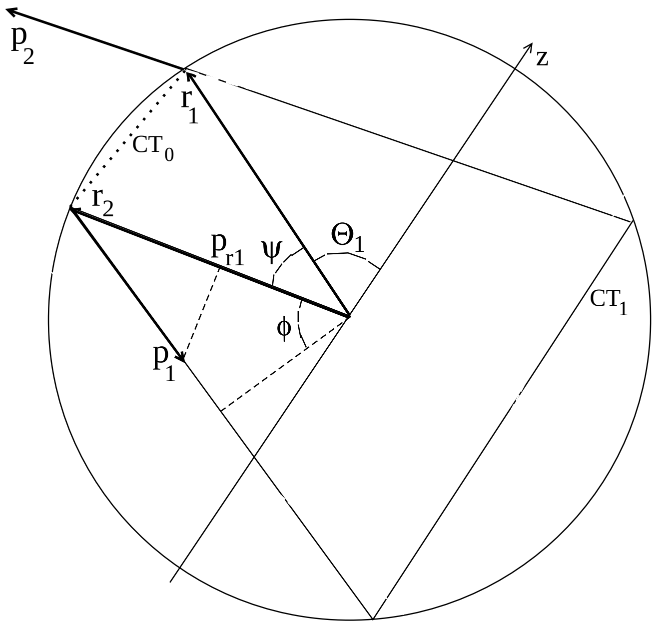

Fig. 4. The trajectories CT_0 and CT_1

$$\mathbf{r}_1\{r_1, \theta_1, \varphi_1\} \Rightarrow \mathbf{r}_2\{r_2, \theta_2, \varphi_2\}$$

CT: $\phi = \phi_{PO} - \frac{\psi}{2v}, \quad \phi_{PO} = \frac{\pi w}{v}$

v is the vertex number and w is the winding number, $\psi = \theta_2 - \theta_1$

$$G = G_{CT_0} + G_{CT_1} \Rightarrow \gamma(\psi) = \gamma_{wf} + \gamma_{corr}$$

$$G_{CT_0} \approx -\left(m/2\pi\hbar^2 r_{12}\right) \exp\left(\frac{i}{\hbar} r_{12} p\right), \quad G_1 = \sum_{CT \neq CT_0} G_{CT}$$

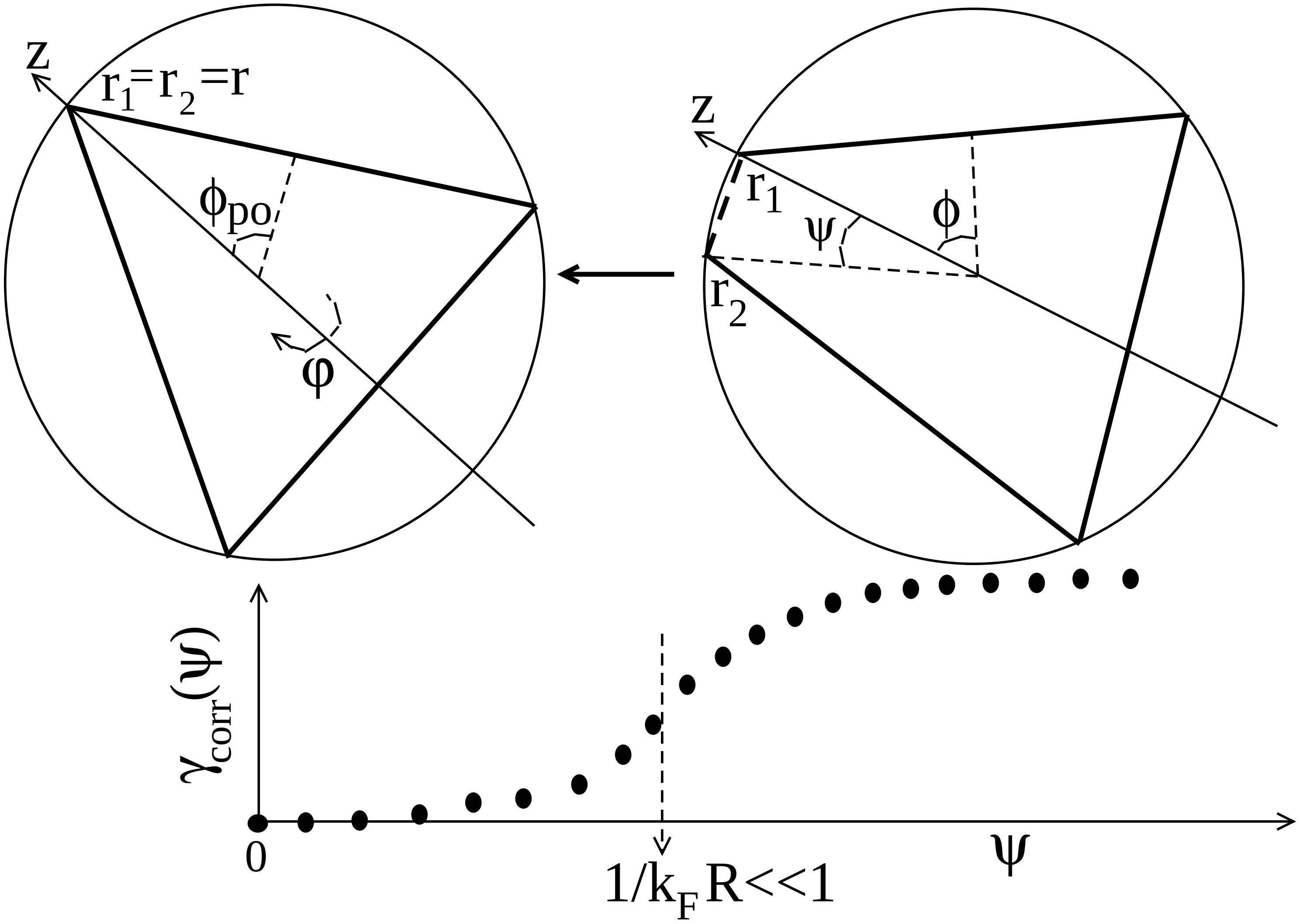

$$\gamma_{corr}(\psi) = \gamma_{wf} \sum_{v,w} \frac{\sin^3\phi \, \cos\phi}{2v\sin\psi} \left[1 - J_0\left(\sqrt{\frac{\Delta S}{\hbar}}\right)\right], \quad \phi = \phi_{PO} - \frac{\psi}{2v}$$

$\Delta S/\hbar = \pi k_F R_0 \cos\phi_{PO} \sin\psi$, $\phi_{PO} = \pi w/v$, **uniform approximation**

by M.Brack, R.K.Bhaduri, Semiclassical physics, 2003

$k_F R \setminus n$	2	3	4	5	6	7	8	9	10
10.0	0.73	1.15	0.92	1.05	0.97	1.02	0.99	1.01	0.99
20.0	0.69	1.20	0.82	1.12	0.82	1.07	0.95	1.04	0.97
30.0	0.84	1.16	0.80	1.14	0.87	1.10	0.91	1.07	0.95
40.0	0.95	1.10	0.86	1.13	0.86	1.11	0.89	1.08	0.93
50.0	0.97	1.06	0.93	1.09	0.88	1.10	0.89	1.09	0.91
∞	1.11	0.92	1.06	0.95	1.08	0.96	1.03	0.97	1.03
K&R	0.00	0.85	0.45	0.90	0.62	0.93	0.71	0.94	0.76

Table: Friction coefficients γ/γ_{wf} vs multipolarity n for small slow. vibrations; K&R is Koonin&Randrup,1977, Abrosimov et al., 1999.

INERTIA: $M(\psi) = M_{ETF}(\psi) + M_{corr}(\psi), \quad \phi = \phi_{PO} - \frac{\psi}{2v}$

$$M_{corr}(\psi) \propto -\sum_{v,w} \frac{\sin^3\phi \, \cos\phi |\sin\phi|}{\sin\psi} \left[1 - J_0\left(\sqrt{\frac{\Delta S}{\hbar}}\right)\right]$$

$k_F R \setminus n$	2	3	4	5	6	7	8	9	10
5	1.4	2.0	2.5	3.6	3.9	5.0	5.3	6.4	6.6
6	1.1	1.5	1.9	2.8	2.9	3.8	4.0	4.8	5.0
7	0.9	1.2	1.5	2.2	2.4	3.1	3.2	3.9	4.0
8	0.8	1.0	1.3	1.9	2.0	2.6	2.7	3.3	3.4
9	0.7	0.9	1.1	1.7	1.7	2.3	2.3	2.9	2.9
10	0.4	0.8	1.0	1.5	1.5	2.0	2.0	2.6	2.6
∞	-1.6	1.9	2.2	-2.2	2.3	-2.3	11	8.8	2.7
K&R		0.05		0.025		0.02		0.015	

Table 1: Inertia M in units of the irrotational flow inertia M_{irr} vs multipolarity n and $k_F R_0$.

CONCLUSIONS

- **Within the response function theory, we derived semiclassically by using the POT the smooth friction and inertia coefficients for slow small-amplitude vibrations near the spherical shape accounting for the nonlocal trajectory corrections.**
- **It was important to solve the fundamental problem of the symmetry breaking related to an appearance of the periodic-orbit families at a spherical equilibrium shape.**
- **The transport coefficients depend essentially on the particle numbers, especially for smaller multipolarities, in contrast to earlier results.**
- **As perspectives, our semiclassical results might be helpful for better understanding the one-body friction and inertia of the nuclear collective dynamics within the Microscopic - Macroscopic Model like in fission and heavy ion collisions.**

THANKS!

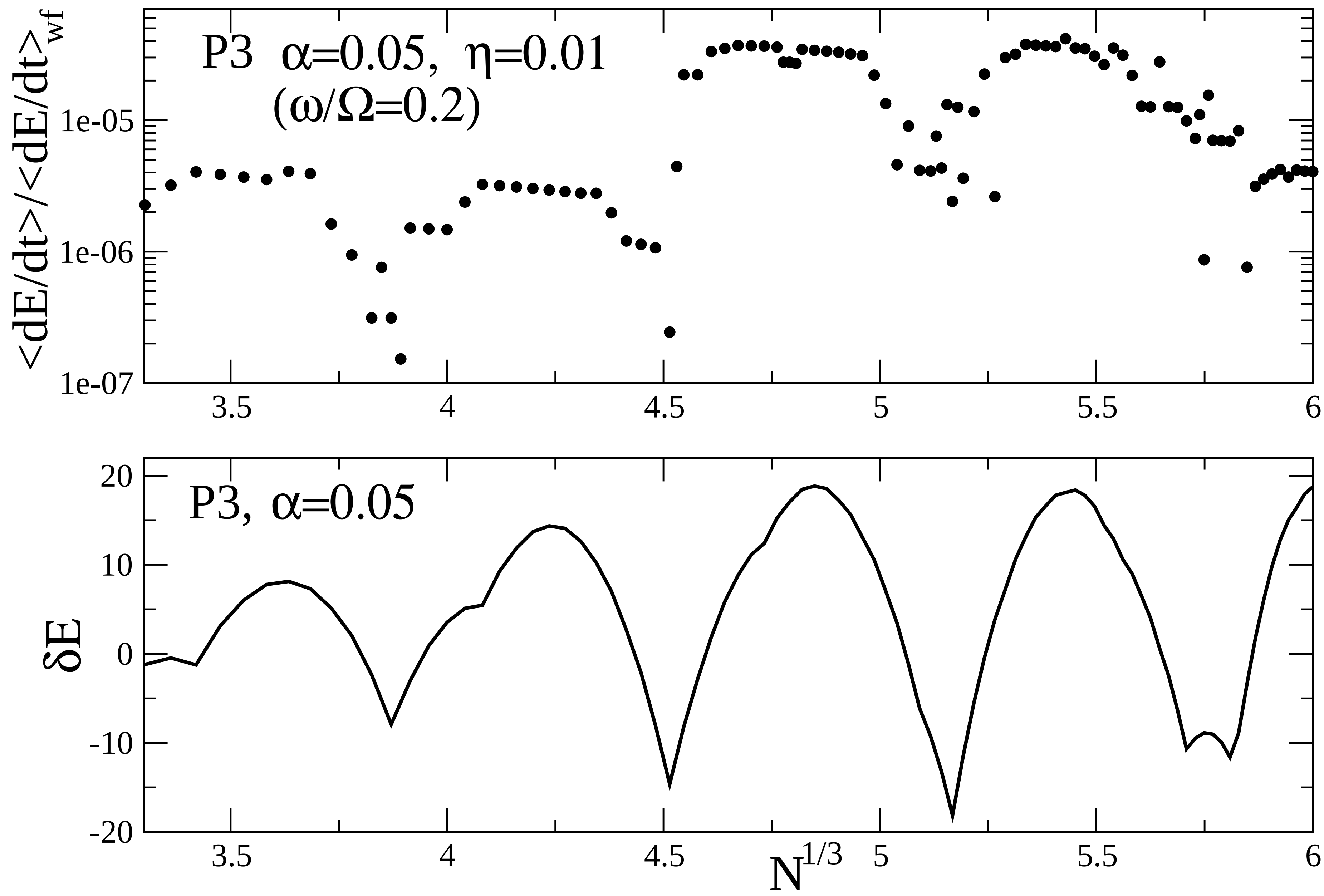

Fig. 11. Mean time derivatives $< dE/dt >$ in the w.f. units (top) and shell corrections δE (bottom) vs. particle numbers, $N^{1/3}$.

SHELL CORRECTIONS

$$\delta E = \sum_{PO} \left(\frac{\hbar}{t_{PO}} \right)^2 \mathcal{B}_{PO} \cos \left[\frac{1}{\hbar} S_{PO}(\varepsilon_F) - \frac{\pi}{2} \mu_{PO} \right], \quad \text{(Strutinsky \& M.,1975,76)}$$

$$\delta\gamma \propto \sum_{CT,CT'} \Upsilon_{CT,CT'} \cos \left\{ \frac{1}{\hbar} \left[S_{CT}(\varepsilon_F) \pm S_{CT'}(\varepsilon_F) \right] \right\}, \quad \hbar\Omega = 2\pi\hbar / t_{CT}$$

$k_F R$ \n	0	1	2	3	4	5	6	7	8	9	10
5.0	0.00	1.31	0.92	1.07	0.98	1.02	0.99	1.01	1.00	1.00	1.00
10.0	0.20	1.35	0.73	1.15	0.92	1.05	0.97	1.02	0.99	1.01	0.99
15.0	0.60	1.29	0.67	1.19	0.86	1.09	0.88	1.04	0.97	1.02	0.99
20.0	0.86	1.22	0.69	1.20	0.82	1.12	0.82	1.07	0.95	1.04	0.97
25.0	0.96	1.16	0.76	1.19	0.80	1.14	0.77	1.08	0.94	1.05	0.97
30.0	0.93	1.19	0.84	1.16	0.80	1.14	0.87	1.10	0.91	1.07	0.95
35.0	0.86	1.10	0.91	1.13	0.83	1.14	0.86	1.11	0.90	1.07	0.94
40.0	0.80	1.09	0.95	1.10	0.86	1.13	0.86	1.11	0.89	1.08	0.93
45.0	0.75	1.09	0.97	1.08	0.89	1.11	0.87	1.11	0.89	1.09	0.92
50.0	0.75	1.09	0.97	1.06	0.93	1.09	0.88	1.10	0.89	1.09	0.91
∞	1.59	0.83	1.11	0.92	1.06	0.95	1.08	0.96	1.03	0.97	1.03
K&R	0.00	0.00	0.00	0.85	0.45	0.90	0.62	0.93	0.71	0.94	0.76

Table: Friction coefficients γ/γ_{wf} vs multipolarity n for small slow. vibrations; K&R is Koonin&Randrup,1977, Abrosimov et al., 1999.

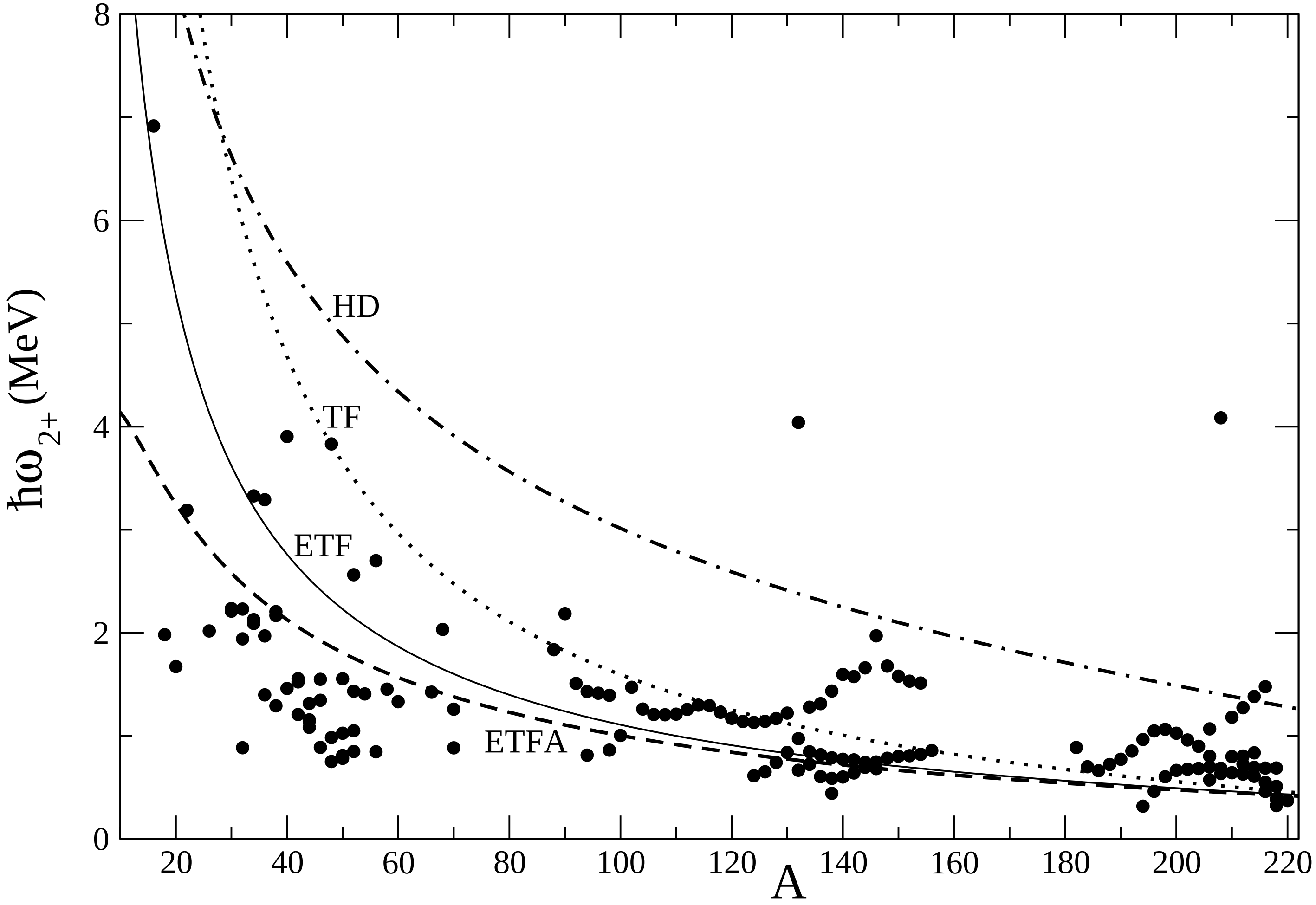

Fig. 2. Low-lying quadrupole vibration energies $\hbar\omega_{2+}$ vs particle number A; frequent dots are TF; thin solid is ETF; thick dashed is ETFA; dash-dotted shows HD. Heavy full dots are the experimental data [Raman, 2001] for nearly spherical nuclei with $q_2 < 0.05$; $\rho = 0.16$ fm^{-3}, $b_v = 16$ MeV, $b_s = 18$ MeV, $K = 220$ MeV, $b_{sym} = 60$ MeV.

$k_F R \backslash n$	0	1	2	3	4	5	6	7	8	9	10
5		2.7	1.4	2.0	2.5	3.6	3.9	5.0	5.3	6.4	6.6
6		2.5	1.1	1.5	1.9	2.8	2.9	3.8	4.0	4.8	5.0
7		2.4	0.9	1.2	1.5	2.2	2.4	3.1	3.2	3.9	4.0
8		2.3	0.8	1.0	1.3	1.9	2.0	2.6	2.7	3.3	3.4
9		2.3	0.7	0.9	1.1	1.7	1.7	2.3	2.3	2.9	2.9
10		2.3	0.4	0.8	1.0	1.5	1.5	2.0	2.0	2.6	2.6
∞		2.0	-1.6	1.9	2.2	-2.2	2.3	-2.3	11	8.8	2.7
K&R		1.00		0.05		0.025		0.02		0.015	

Table 2: Inertia M in units of the irrotational flow inertia M_{irr} vs multipolarity n and $k_F R_0$.

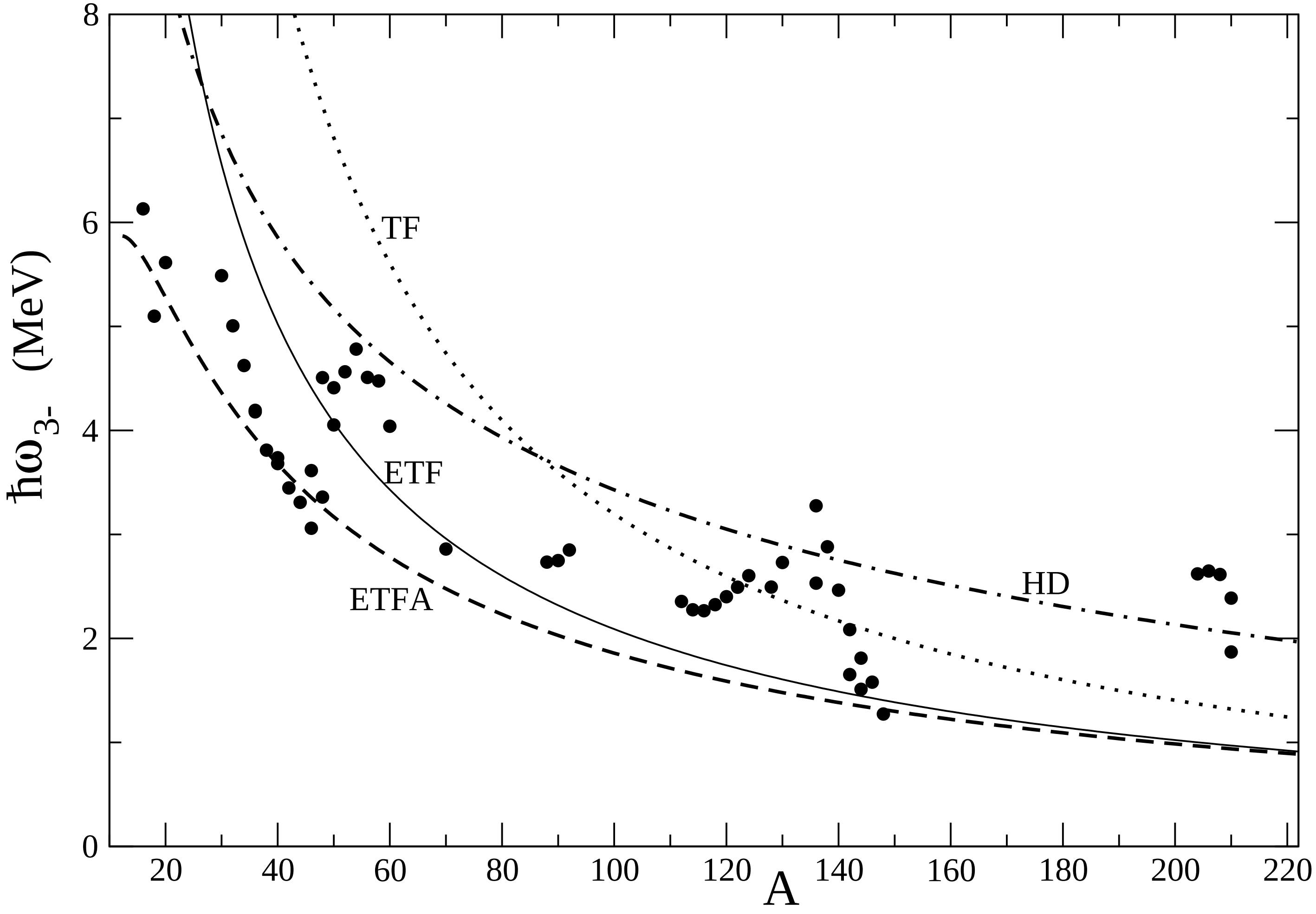

Fig. 3. The same for the low-lying octupole vibration energies $\hbar\omega_{3-}$; the experimental data are taken from [Kibedi, 2005].

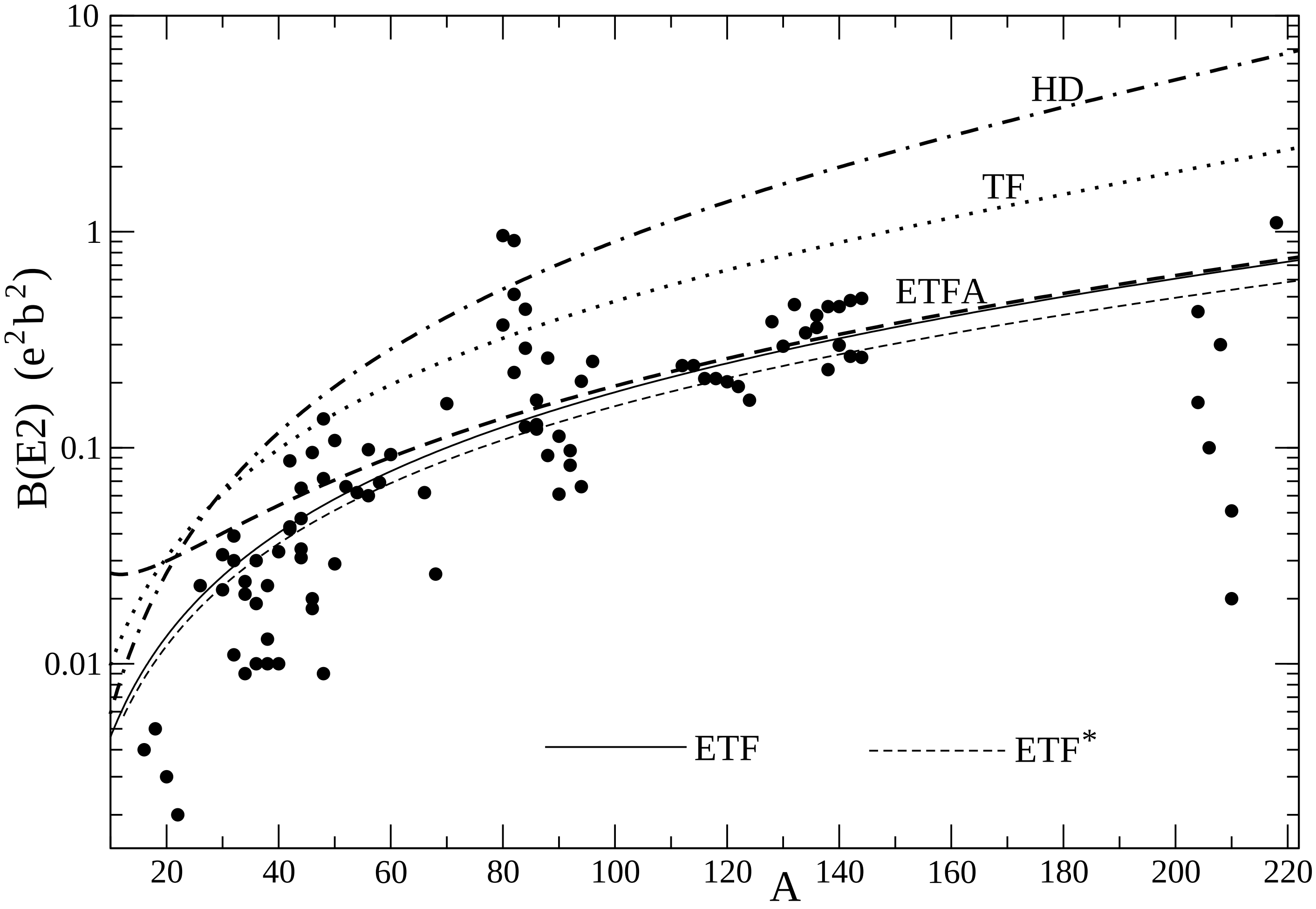

Fig. 4. The reduced probabilities B(E2) in units of e^2 b^2; full heavy points are experimental data [Raman, 2001]; frequent dashed is semiclassical $\boldsymbol{B(E2)}$ with (solid) and without (dashed) account for the $\boldsymbol{\eta}$ dependence; other notations are the same as in Fig. 2.

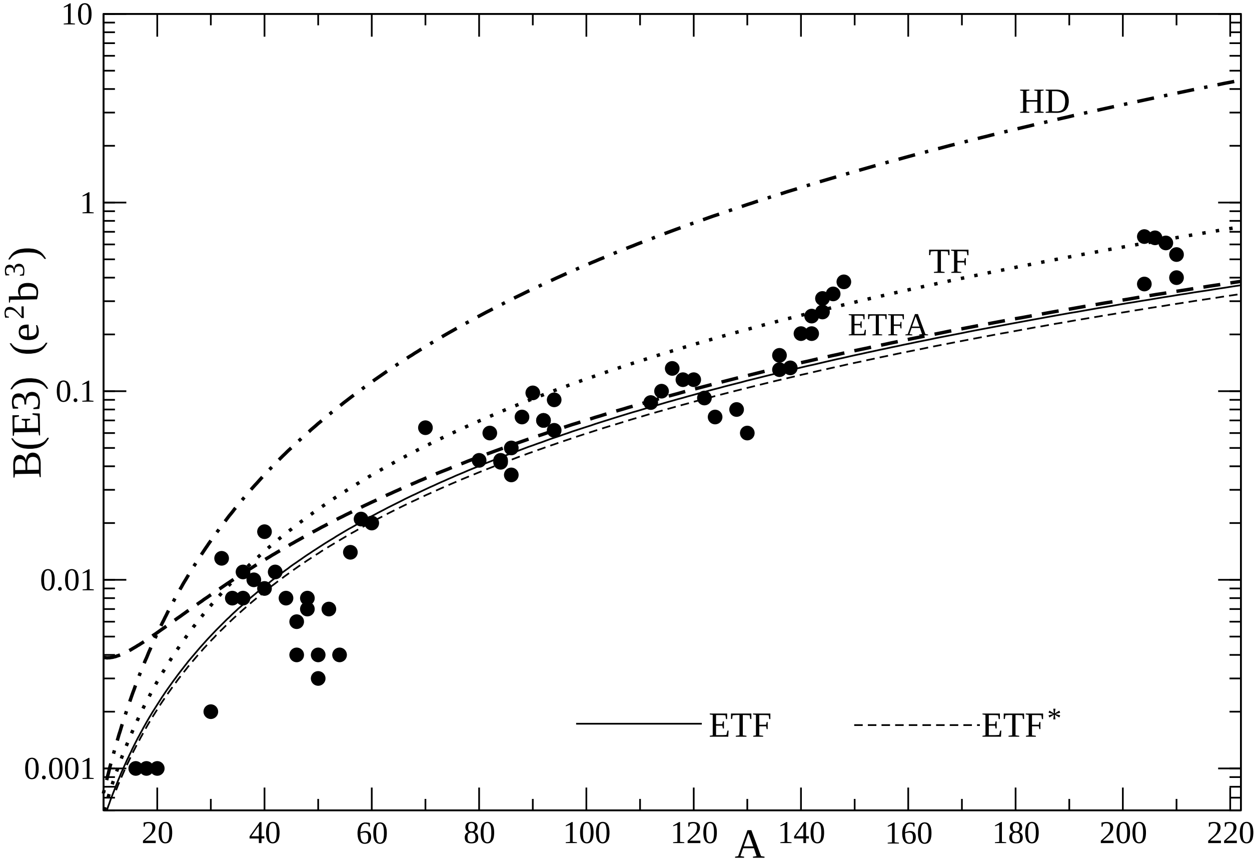

Fig. 5. The reduced transition probabilities $\boldsymbol{B(E3)}$ in units of $e^{\mathbf{2}}$ $b^{\mathbf{3}}$; full heavy points are experimental data [Kibedi, 2005]; other notations are the same as in Fig. 4.

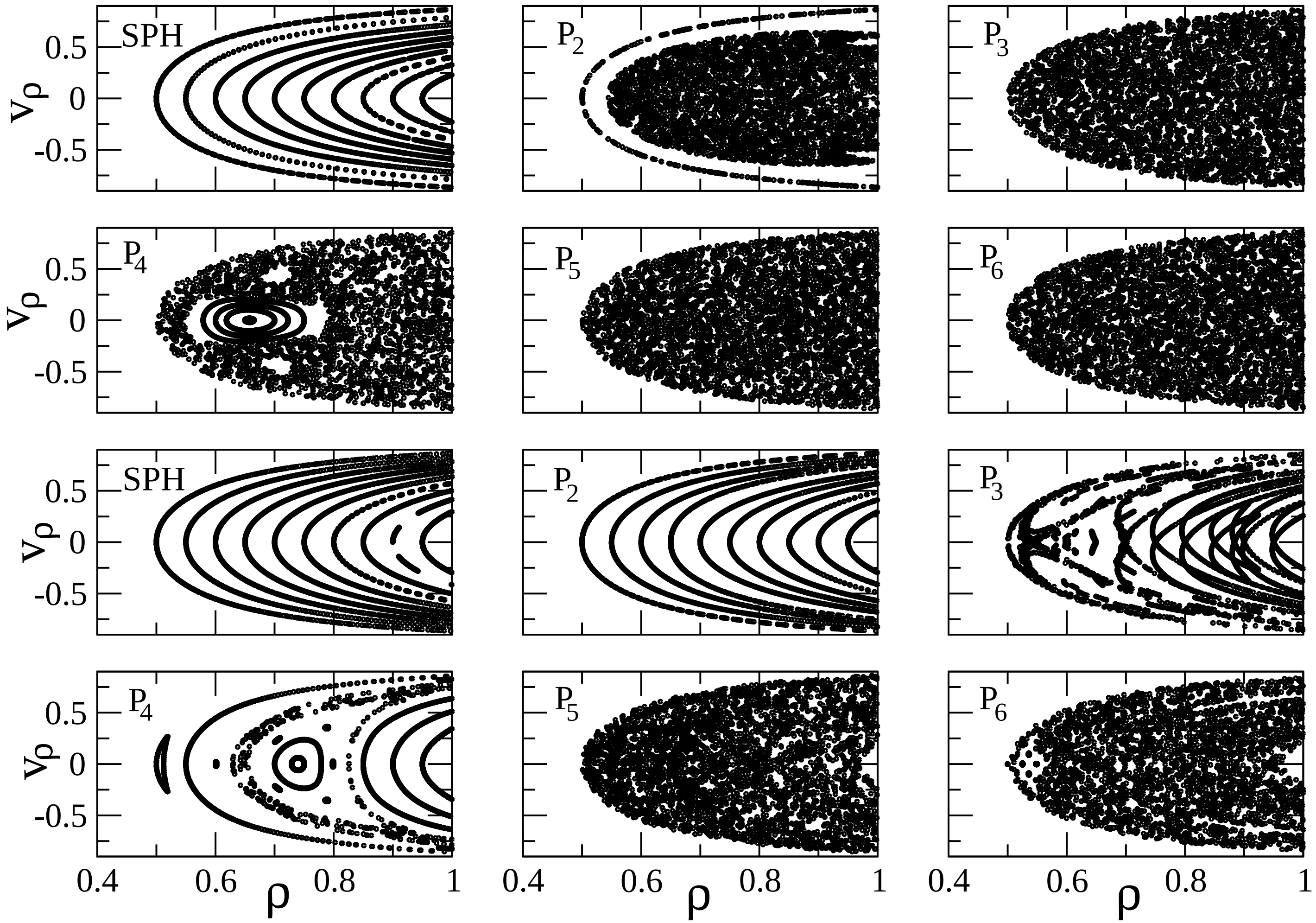

Fig.4. Poincare sections for six shapes at the deformation $\alpha = 0.05$ (two lower rows) and deformation $\alpha = 0.4$ (two upper rows) for the projections of the angular momentum on the symmetry axis $K = 0.5$ with respect to the maximal value

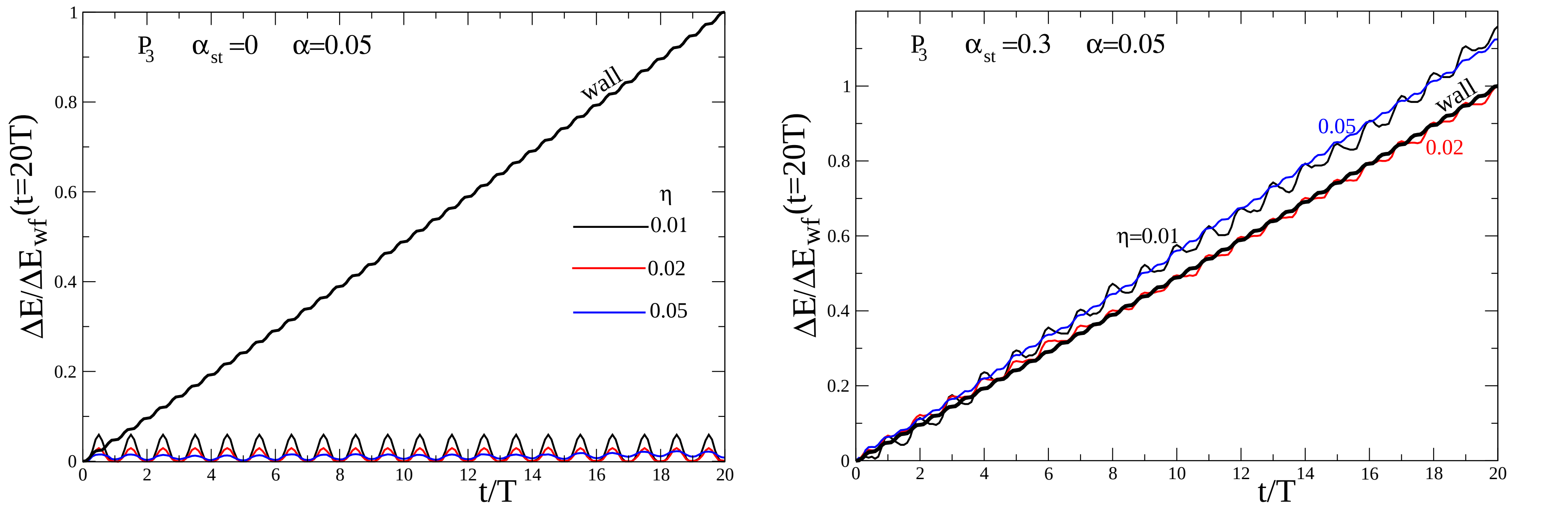

Fig.6. The classical dynamical excitations $\boldsymbol{\Delta E}$ in units of the wall formula value $\boldsymbol{\Delta E_{wf}(t = 20T)}$ as functions of the time $\boldsymbol{t}$ in units of the period $\boldsymbol{T = 2\pi\alpha/\eta}$ for vibrations near the spherical ($\boldsymbol{\alpha_{st} = 0}$, left) and deformed ($\boldsymbol{\alpha_{st} = 0.3}$, right) shapes of the cavity